

COMPUTATIONS OF TURBULENT FLOW CHARACTERISTICS AND HEAT  
TRANSFER ON FORWARD-FACING STEPS

حساب خواص السريان الاضطرابي وانتقال الحرارة على السطح الامامي لجسم عارض

A.A. El-Hadik and M.Y. Salam\*

Mechanical Engineering Department,  
Faculty of Technological Studies, Kuwait

\*Mechanical Engineering Department,  
College of Engineering & Petroleum  
Kuwait University, Kuwait

المخلاصة :

=====  
يتناول هذا البحث دراسة خواص السريان وانتقال الحرارة في حالة السريان التدويري الاضطرابي على سطح الوجه الامامي لجسم عارض وذلك عن طريق التحليل النظري .  
في هذا البحث استخدم النموذج المعروف (  $k - \epsilon$  ) وأخذ في الاعتبار ان توزيع الدوامات تأخذ شكلا خطيا بجوار سطح الجسم العارض . ولقد روعي تطوير نموذج (  $k - \epsilon$  ) لتتمكن من حساب قيم كل من منحنيات خطوط السريان واجهادات رينولدز .  
ولقد أمكن استنتاج قيم كل من معامل انتقال الحرارة وخطوط السريان وخطوط درجات الحرارة اللاعددية وخطوط السرعة وطاقة الاضطراب وذلك لقيم مختلفة لرقم رينولدز وعند ارتفاعات متفيدة على سطح الجسم العارض . وقد أظهرت النتائج في هذا البحث ان ارتفاع سطح الجسم العارض يؤثر سلبا على حجم وموضع منطقة الانفصال ونقطة إعادة التلامس . كما تبين ايضا ان انتقال الحرارة يزداد مع زيادة ارتفاع السطح العارض . كما وأن خطوط قيم درجات الحرارة اللاعددية تنقل كثيرا وتقترب من السطح عند الارتفاعات الكبيرة .

**ABSTRACT** - Numerical calculations of heat transfer and flow field characteristics of turbulent recirculating flows on forward-facing steps are presented in this paper. The calculations are based on the (k -  $\epsilon$ ) model. In the vicinity of the wall a linear vorticity distribution model was used. The (k -  $\epsilon$ ) model has improved to account for the streamline curvature and the Reynolds stresses, and the computer program was also improved with a finite difference and iterative technique.

The present results include computed heat transfer coefficients, streamlines and isothermal lines, velocity profiles and kinetic energy distributions at different Reynolds numbers and different step heights.

One of the significant results in this study is the influence of the step height on the size and location of the separation region and reattachment point. It was found that the heat transfer mechanism is positively influenced by larger step sizes. The size of the isothermal lines becomes smaller and closer to the wall by larger steps. This result is noticed both upstream and downstream of the step.

## INTRODUCTION

One of the most important aspects of turbulent flow is that which occurs at or near separation. Besides being an important basic science, the problem of separated flow and recirculation finds a lot of engineering applications. The effective design of many thermal process components depends thoroughly on the recognition and accounting for the role of turbulent motion immediately adjacent to the wall. On a larger scale recirculating flow plays an important role in building aerodynamics. The effective study of disturbing winds in ground levels among building depends crucially on recognition of the vortices formed by recirculating flows on the walls and roofs.

The presence of a recirculating wall boundary layer greatly influences the process of heat transfer in separated flows. It has been shown experimentally that the heat transfer coefficients are considerably larger than those on attached boundary layers. The increase in the convective heat transfer process can be explained, in principle, as being due to the increase in streamwise turbulent kinetic energy in the mixing layer.

The problem of flow characteristics and heat transfer in recirculating flows has taken a good share in literature. References [1] - [3] are some of the important research works in this field. The problem of forward facing steps finds less interest in the literature although it has many engineering applications. Correlations of experimental and numerical data on turbulent recirculating flows over over steps remains scarce indeed. However, the fundamentals of the numerical technique for this and similar problems has been well established. Gosman et.al. [4] proposed in details the fundamentals of the computations of recirculating flows. W. Frost et.al. [5] analyzed the atmospheric flow over a two-dimensional forward-facing step, using a  $k-\epsilon$  computational model. Lakshminarayana [6] gave a review of different turbulence models comparing the various methods available to predict such flows and their performance. The  $k-\epsilon$  model was given a critical emphasis in a study by Rodi, W. [7].

The present work handles the problem of fluid flow and heat transfer together over a forward facing step. The computations are done for variable Reynolds numbers and on different step heights using the  $k-\epsilon$  computational model. The flow field includes turbulent velocity profiles before the step, turbulent separation and recirculation over the step and reattachment of the flow down stream from the step. The thermal field analyzed assumes a constant heat current such that the temperature gradient ( $dT/dx$ ) in flow direction is very small. The purpose of the paper is to present the results obtained by applying the  $k-\epsilon$  model over forward facing steps. numerically analyzing both the flow field and the thermal field.

## COMPUTATIONAL MODEL

In the following paragraphs only a brief outline of the mathematical model and computational procedures are given. Full details are given in references [1,4,5]. Figure (1) shows the forwardfacing step with the numerical model superimposed on it. The grid is non uniform as shown. The coordinate system was chosen such that the origin was located at the lower step corner with the positive x-axis pointing in the downstream direction. The y-axis is normal

to the surface of the plate parallel to the step wall. In this coordinate system the flow field extends and covers 11 times the step height in the downstream and upstream direction, and about 10 times in the vertical direction.

### GOVERNING EQUATIONS

The turbulent mean flow equations for a two-dimensional flow field are those for momentum .

$$\rho \left( \mu \frac{\partial u}{\partial x} + \nu \frac{\partial u}{\partial y} \right) = -\frac{\partial p}{\partial x} + \mu \left( \frac{\partial^2 u}{\partial x^2} + \frac{\partial^2 u}{\partial y^2} \right) - \rho \left( \overline{\frac{\partial u'^2}{\partial x}} + \overline{\frac{\partial u'v'}{\partial y}} \right) \quad \dots (1)$$

$$\rho \left( u \frac{\partial v}{\partial x} + \nu \frac{\partial v}{\partial y} \right) = -\frac{\partial p}{\partial y} + \mu \left( \frac{\partial^2 v}{\partial x^2} + \frac{\partial^2 v}{\partial y^2} \right) - \rho \left( \overline{\frac{\partial v'^2}{\partial x}} + \overline{\frac{\partial v'u'}{\partial y}} \right) \quad \dots (2)$$

continuity

$$\frac{\partial (\rho u)}{\partial x} + \frac{\partial (\rho v)}{\partial y} = 0 \quad \dots (3)$$

stream function  $\Psi$

$$\rho u = \frac{\partial \Psi}{\partial y} \quad \text{and} \quad \rho v = -\frac{\partial \Psi}{\partial x} \quad \dots (4)$$

vorticity  $\omega$

$$\omega = \frac{\partial v}{\partial x} - \frac{\partial u}{\partial y} \quad \dots (5)$$

thermal energy

$$\rho u \frac{\partial T}{\partial x} + \rho v \frac{\partial T}{\partial y} = \left( \frac{\mu}{Pr_t} + \frac{\mu_t}{Pr_t} \right) \left( \frac{\partial^2 T}{\partial x^2} + \frac{\partial^2 T}{\partial y^2} \right) \quad \dots (6)$$

turbulence energy

$$\rho u \frac{\partial k}{\partial x} + \rho v \frac{\partial k}{\partial y} = \frac{\partial}{\partial x} \left[ \left( \mu + \frac{\mu_t}{\sigma_k} \right) \frac{\partial k}{\partial x} \right] + \frac{\partial}{\partial y} \left[ \left( \mu + \frac{\mu_t}{\sigma_k} \right) \frac{\partial k}{\partial y} \right] + \mu_t G - \rho \varepsilon = 0 \quad \dots (7)$$

turbulence dissipation rate

$$\rho u \frac{\partial \varepsilon}{\partial x} + \rho v \frac{\partial \varepsilon}{\partial y} = \frac{\partial}{\partial x} \left[ \left( \mu + \frac{\mu_t}{\sigma_\varepsilon} \right) \frac{\partial \varepsilon}{\partial x} \right] + \frac{\partial}{\partial y} \left[ \left( \mu + \frac{\mu_t}{\sigma_\varepsilon} \right) \frac{\partial \varepsilon}{\partial y} \right] + \frac{C_1 \varepsilon \mu_t}{k} - \frac{\rho C_2 \varepsilon^2}{k} \quad \dots (8)$$

where

$$G = 2 \left[ \left( \frac{\partial u}{\partial x} \right)^2 + \left( \frac{\partial v}{\partial y} \right)^2 \right] + \left( \frac{\partial u}{\partial y} + \frac{\partial v}{\partial x} \right)^2 \quad \dots (9)$$

and the turbulent viscosity  $\mu_t$  is given by

$$\mu_t = C_u \rho k^2 / \varepsilon = \overline{\rho w'v'} / \left( \frac{\partial u}{\partial y} \right)^2, \quad \dots (10)$$

the constants are

| $C_1$ | $C_2$ | $C_u$ | $\sigma_k$ | $\sigma_\varepsilon$ | $\sigma_t$ |
|-------|-------|-------|------------|----------------------|------------|
| 1.4   | 2.0   | 0.07  | 1.0        | 1.3                  | 0.9        |

The heat transfer coefficient can be calculated from

$$q_w = -\lambda \frac{\partial T}{\partial y} \Big|_{y=0} = h (T_w - T_\infty), \quad \dots (11)$$

which gives

$$h = -\lambda \frac{\partial T}{\partial y} \Big|_{y=0} / (T_w - T_\infty) \quad \dots (12)$$

When the momentum equations (1) and (2) are differentiated with respect to  $Y$  and  $x$  respectively, the resultant equation is substituted in (3) with (4) and (5) to Yield the vorticity equation in th from

$$\frac{\partial}{\partial x} \left( \frac{\partial \psi}{\partial y} \right) - \frac{\partial}{\partial y} \left( \frac{\partial \psi}{\partial x} \right) - \frac{\partial}{\partial x} \left( \omega \frac{\partial \omega}{\partial x} \right) - \frac{\partial}{\partial y} \left( \omega \frac{\partial \omega}{\partial y} \right) + d = 0 \quad \dots (13)$$

$$\text{where } d = \frac{\partial}{\partial x} \left[ \rho \left( \frac{\partial}{\partial y} v'^2 + \frac{\partial}{\partial x} \overline{u'v'} \right) \right] - \frac{\partial}{\partial y} \left[ \rho \left( \frac{\partial}{\partial x} \overline{u'^2} + \frac{\partial}{\partial y} \overline{u'v'} \right) \right]$$

Substituting equations (3), (4) and (5) yield

$$\frac{\partial^2 \psi}{\partial x^2} + \frac{\partial^2 \psi}{\partial y^2} + \rho \omega = 0 \quad \dots (14)$$

equations (3), (4) and (6) give the thermal energy equation in the form

$$\frac{\partial}{\partial x} \left( T \frac{\partial \psi}{\partial y} \right) - \frac{\partial}{\partial y} \left( T \frac{\partial \psi}{\partial x} \right) - \frac{\partial}{\partial x} \left[ \left( \frac{\mu_t}{\rho r_t} + \frac{\mu}{\rho r} \right) \frac{\partial T}{\partial x} \right] - \frac{\partial}{\partial y} \left[ \left( \frac{\mu_t}{\rho r_t} + \frac{\mu}{\rho r} \right) \frac{\partial T}{\partial y} \right] = 0 \quad \dots (15)$$

The turbulence energy equation is obtained from equations (3), (4) and (7) in the form.

$$\frac{\partial}{\partial x} \left( k \frac{\partial \Psi}{\partial y} \right) - \frac{\partial}{\partial y} \left( k \frac{\partial \Psi}{\partial x} \right) - \frac{\partial}{\partial x} \left[ \left( \mu + \frac{\mu_t}{\sigma_k} \right) \frac{\partial k}{\partial x} \right] - \frac{\partial}{\partial y} \left[ \left( \mu + \frac{\mu_t}{\sigma_k} \right) \frac{\partial k}{\partial y} \right] - \mu_t G + \rho \varepsilon = 0 \quad (16)$$

The equation for the dissipation rate is then given as

$$\frac{\partial}{\partial x} \left( \varepsilon \frac{\partial \Psi}{\partial y} \right) - \frac{\partial}{\partial y} \left( \varepsilon \frac{\partial \Psi}{\partial x} \right) - \frac{\partial}{\partial x} \left[ \left( \mu + \frac{\mu_t}{\sigma_\varepsilon} \right) \frac{\partial \varepsilon}{\partial x} \right] - \frac{\partial}{\partial y} \left[ \left( \mu + \frac{\mu_t}{\sigma_\varepsilon} \right) \frac{\partial \varepsilon}{\partial y} \right] - \frac{C_1 \varepsilon_u G}{k} + \frac{\rho C_2 \varepsilon^2}{k} = 0 \quad \dots (17)$$

The mathematical problem posed in this paper relies on the solution suggested by Gossman et al [4]. The solution algorithm utilizes the stream function and the vorticity variables. The governing equations for the stream function, vorticity, thermal energy, kinetic energy and rate of dissipation are cast in an elliptical partial differential equation suitable for simultaneous numerical integration. This differential equation is then replaced by integration over finite areas. The asymptotic functions a, b, c, d are given in table (1) as follows :

| Q             | a | b   | c | d  |
|---------------|---|---|---|--|
| $\omega$      | 1 | $\mu$   | 1 | $\frac{\partial}{\partial x} \left[ \rho \left( \frac{\partial \overline{v'^2}}{\partial y} + \frac{\partial \overline{u'v'}}{\partial x} \right) \right]$<br>$-\frac{\partial}{\partial y} \left[ \left( \frac{\partial \overline{u'^2}}{\partial x} + \frac{\partial \overline{v'u'}}{\partial y} \right) \right]$ |
| $\Psi$        | 0 | 1   | 1 | $-\rho \omega$   |
| T             | 1 | $\frac{\mu_t}{\rho Pr_t} + \frac{\mu}{\rho Pr}$ | 1 | 0  |
| K             | 1 | $\frac{\mu_t}{\sigma_k} + \mu$                  | 1 | $-\mu_t G + \rho \varepsilon$  |
| $\varepsilon$ | 1 | $\mu + \frac{\mu_t}{\sigma_\varepsilon}$        | 1 | $\frac{\rho C_2 \varepsilon^2}{k} - C_{1\varepsilon} \mu_t G$  |

Table 1. Functional constants a, b, c, d

#### BOUNDARY CONDITIONS

The nature of the complicated present problem dictates that boundary conditions are prescribed along the entire boundary of the flow region. Following Fig. (2) along the inlet, the outlet and the upper and lower boundaries, the boundary conditions were implemented as follows .

#### Inlet and Outlet

The grid system utilized is so large that it is assumed the wall boundary layer is

only a small portion of the flow region subject to analysis. Thus it is taken that free stream velocities  $U_\infty$  and free stream temperature  $T_\infty$  are at inlet and outlet. The maximum vertical distance at inlet  $Y_1$  is of a definite ratio to the maximum vertical distance  $Y_2$  at outlet, such that the continuity equation remains satisfied.

#### Upper face

The location of the upper boundary was assumed far enough that streamline deflections caused by the step were negligibly small. Consequently  $v = 0$ ;  $u = U_\infty$ ,  $T = T_\infty$ ,  $\partial\psi/\partial x = 0$  and  $\psi = U_\infty \cdot Y$  ( $NN_1$ ), where ( $Y$  ( $NN_1$ )) is the highest mode in the grid in the vertical direction.

The turbulent kinetic energy is given as

$$k = (0.1)^2 * (1.5 U_\infty^2),$$

and

$$\partial k / \partial x = 0$$

The rate of dissipation of energy is given as

$$\varepsilon = (0.1)^2 * (1.5)^{0.6} * U_\infty^2 / (0.44 Y (NN_1))$$

#### Lower face

As the free stream is parallel to the solid boundary, the stream function is zero at the wall  $\psi_w = 0$ . The vorticity is more complicated since it derives essentially the flow. According to [5]

$$\omega = \frac{-3 (\psi_b - \psi_w)}{Y^2 (b)},$$

where the subscript  $w$  means the wall, and  $b$  means the second mode from the wall in  $Y$ -direction.

## RESULTS AND CONCLUSIONS

In this study numerical calculations were made using the  $k-\varepsilon$  model for a turbulent flow field and heat transfer around a forward facing step. Three step heights were investigated

$$H = 0.0102 \text{ m}; \quad H = 0.0236 \text{ m}; \quad H = 0.0406 \text{ m}.$$

The free stream velocity was kept constant  $U_\infty = 24 \text{ m/s}$ . The results are presented in figures 3 - 12 in a non-dimensional parameteric form. The Reynolds number and the Nusselt number were taken with respect to the step height  $H$ . Thus the variables reduce to  $x/H$ ;  $Y/H$ ;  $Re = \frac{U_\infty \cdot H}{\nu}$  and  $Nu = \frac{h \cdot H}{k}$

Figures 3, 4 and 5 show the streamline ( $\psi$ ) patterns for the three different step heights  $H/Y_1 = 0.051, 0.118$  and  $0.203$ , i.e. for three different Reynolds numbers. Comparing the various streamline patterns one notices that there are two main separation regions (recirculating vortices) around the step, one vortex upstream and one vortex downstream the step. The

shapes and sizes of these vortices vary in vertical and horizontal distances from the step. It is clear from the figures that the aft vortices behave in a different manner than the front ones. In front of the step the smaller vortices belong to larger steps, whereas the larger aft vortices belong to the larger step heights. This means that the height of the step has a negative effect on the size of the separation region upstream, but a positive effect on that downstream of the step.

In the same figures (3-5) isothermal ( $\theta$ ) lines are plotted, for the same Reynolds numbers. The figures show clearly two distinct isothermal regions upstream and downstream the step. The size of the vortex becomes smaller with larger heights of the step. This is true for both front and aft isothermal regions. Physically this is explained by larger heat transfer in the separation region. When the isothermal region is small it means that it lies closer to the wall and this helps in the heat transfer process. This physical conclusion is further explained in figures 11 and 12.

Figures 6, 7 and 8 show the velocity profiles for different step heights  $H/Y_1 = 0.051$ , 0.118 and 0.203. The velocity distribution gives more information about the separated regions than the stream functions. The amount of overshoot and the size of the back flow are very clearly shown in these profiles.

The turbulent kinetic energy contours in figures 9 and 10 reveal that the turbulence kinetic energy level in the shear layer grows from the step corner. One notices that high turbulence intensity extends throughout a region of 1 to 2 times the step height above the surface. It decays however downstream from the step, as the flow goes over in the flat plate boundary layer.

In figures 11 and 12 the variation of the Nusselt number along the entire flow field is represented. The heat transfer characteristics seem rather complicated in the separated regions. Nevertheless they indicate an increase of heat transfer around the step.

In figure (11) the Nusselt number at a step height  $H/Y_1 = 0.051$  is plotted for three different free stream velocities. It is noticed that the heat transfer coefficient increases as the Reynolds number increases. It has two maxima before and after the step. This result harmonizes with the conclusive remarks given in discussing the isothermal lines.

In figure (12) the Nusselt number variation is presented for the same free stream velocities  $U_\infty = 12$ ; 18 and 24 m/s as in figure (11), for a step height of  $H/Y_1 = 0.203$ . The resulting plots are very similar to those of Fig. (11). However, the Nusselt number reaches higher values (almost twice) than those with the lower step. The maxima of the curves are away from the corner of the step, one upstream and one downstream.

It is worth mentioning that the computational analysis for both flow field and heat transfer is very complicated, yet the results are very encouraging. The authors feel however that some more serious works are needed to apply the  $K - \epsilon$  model for walls with more complex geometry.

#### NOMENCLATURE

a, b, c = functional constants in transport equations, given in table (1).

|            |   |
|------------|---|
| $C_1, C_2$ | = asymptotic constants contained in transport equations.        |
| $C$        | = Pressure coefficient  |
| $C_p$      | = Asymptotic constant in equation (10)                          |
| $d^u$      | = Source term in vorticity equation                             |
| $G$        | = Coefficient variable in equation for turbulent kinetic energy |
| $h$        | = heat transfer coefficient                                     |
| $H$        | = step height   |
| $k$        | = turbulence kinetic energy                                     |
| $T$        | = temperature   |
| $Y_1$      | = maximum vertical distance at inlet to grid system             |
| $Y_2$      | = maximum vertical distance at outlet from grid system          |
| $\mu$      | = dynamic viscosity of fluid                                    |
| $\nu$      | = kinematic viscosity of fluid                                  |
| $\rho$     | = density of fluid  |
| $\epsilon$ | = dissipation rate function                                     |
| $\psi$     | = stream function   |
| $\theta$   | = isothermal function   |
| $w$        | = vorticity function  |

## REFERENCES

- [1] Gooray A. M., Watkins C. B., Wing Aung: Turbulent Heat Transfer Computations for Rearward-Facing Step And Sudden Pipe Expansions, Transactions of the ASME, J. of Heat Transfer, 107, (1985).
- [2] Calenligil M.C., Mellor C.L. : Numerical Solutions of Two-Dimensional Turbulent Separated Flows Using A Reynolds Stress Closure Model, Transactions of ASME, J. Of Fl. Engineering Vol. 107, (1985).
- [3] Moss W.D., Baker S., and Bradbury L.J.S. : Measurements of Mean velocity and Reynolds Stress in Some Regions of Recirculating Flows, First International Symposium on Turbulent Shear Flows, Pennsylvania State University, USA (1977).
- [4] Gosman A.D., Pun W.M., Runchal A.K., Spalding B.D., Wolfstein M. : Heat and Mass Transfer in Recirculating Flows. Academic Press, (1969).
- [5] Frost W., Bitte J. and Chih Fang Shieh: Analysis of Naturally Stable Atmospheric Flow Over a Two-Dimensional Forward-Facing Step, AIAA Journal, Vol. 18, No. 1 (1980).
- [6] Lakshminarayana. B. : Turbulence Modeling for Complex Shear Flows, AIAA J. Vol. 24, (1986).
- [7] Rodi W. : Examples of Turbulence Models for Incompressible Flow, AIAA J. Vol. 20, 1982.



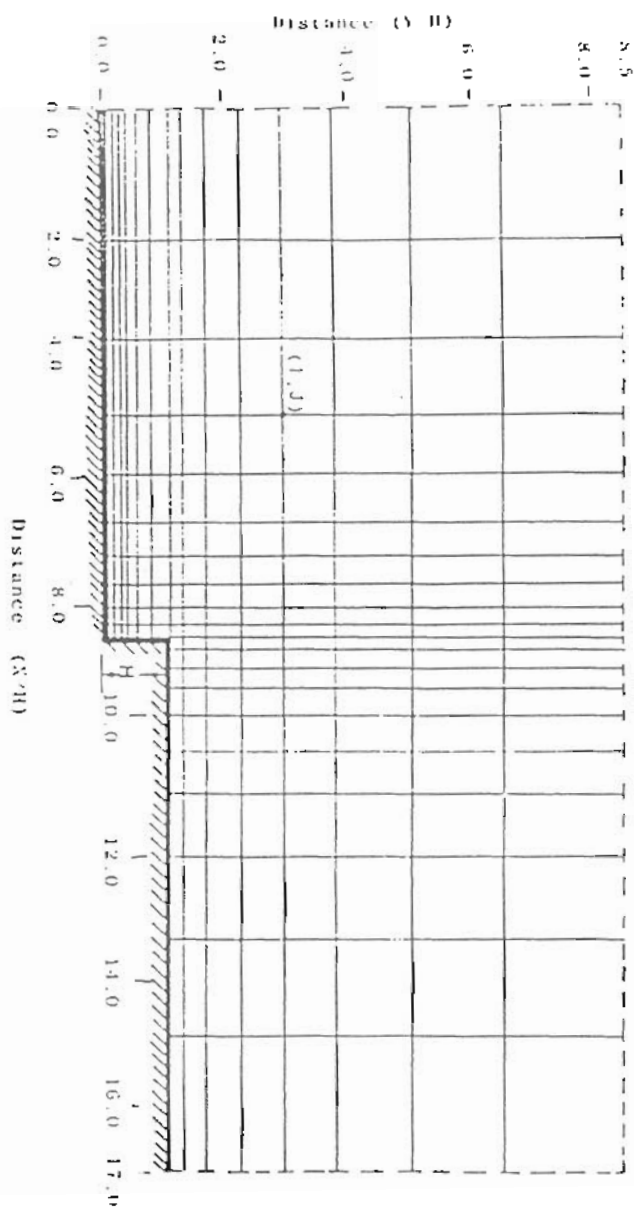


Fig. 1 Computational model over flow region

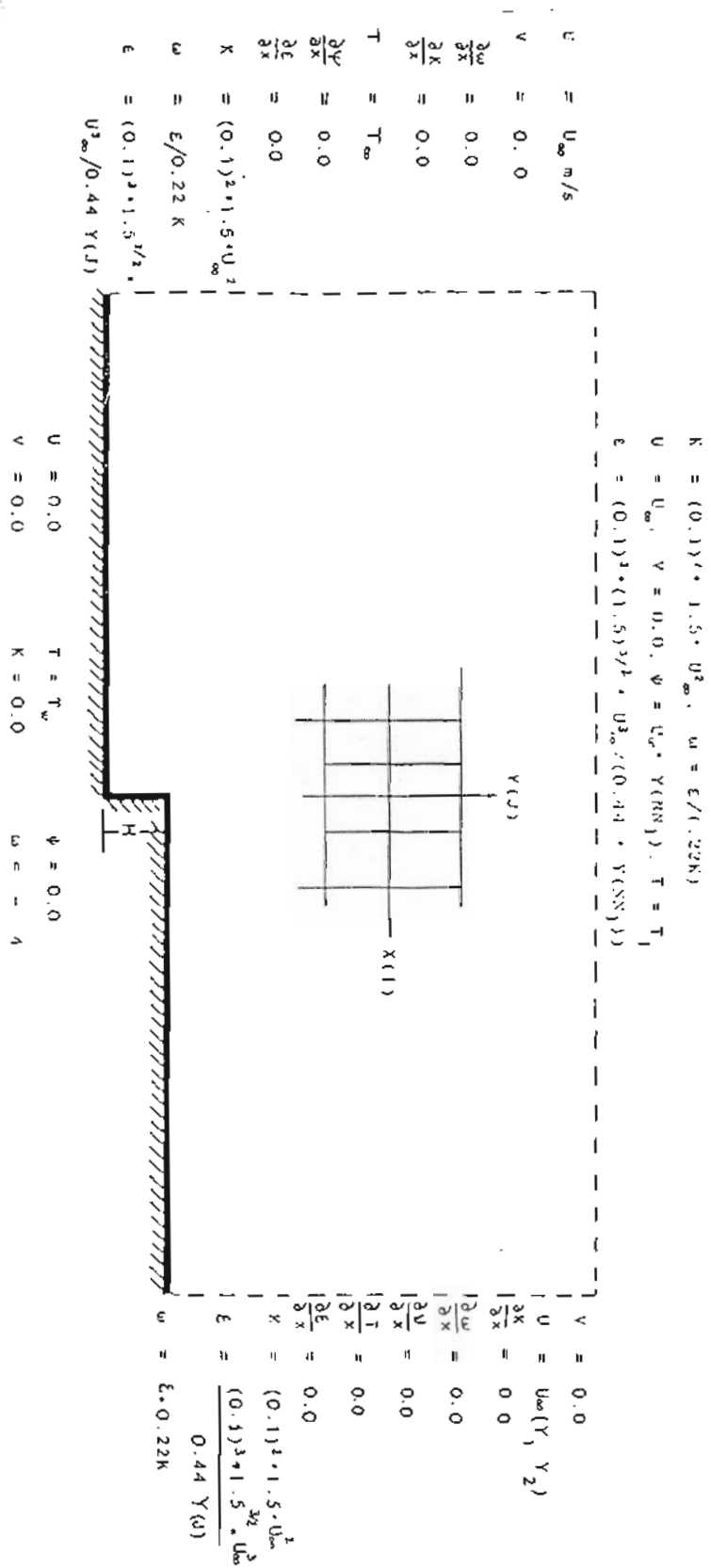


Fig. 2 Boundary Conditions

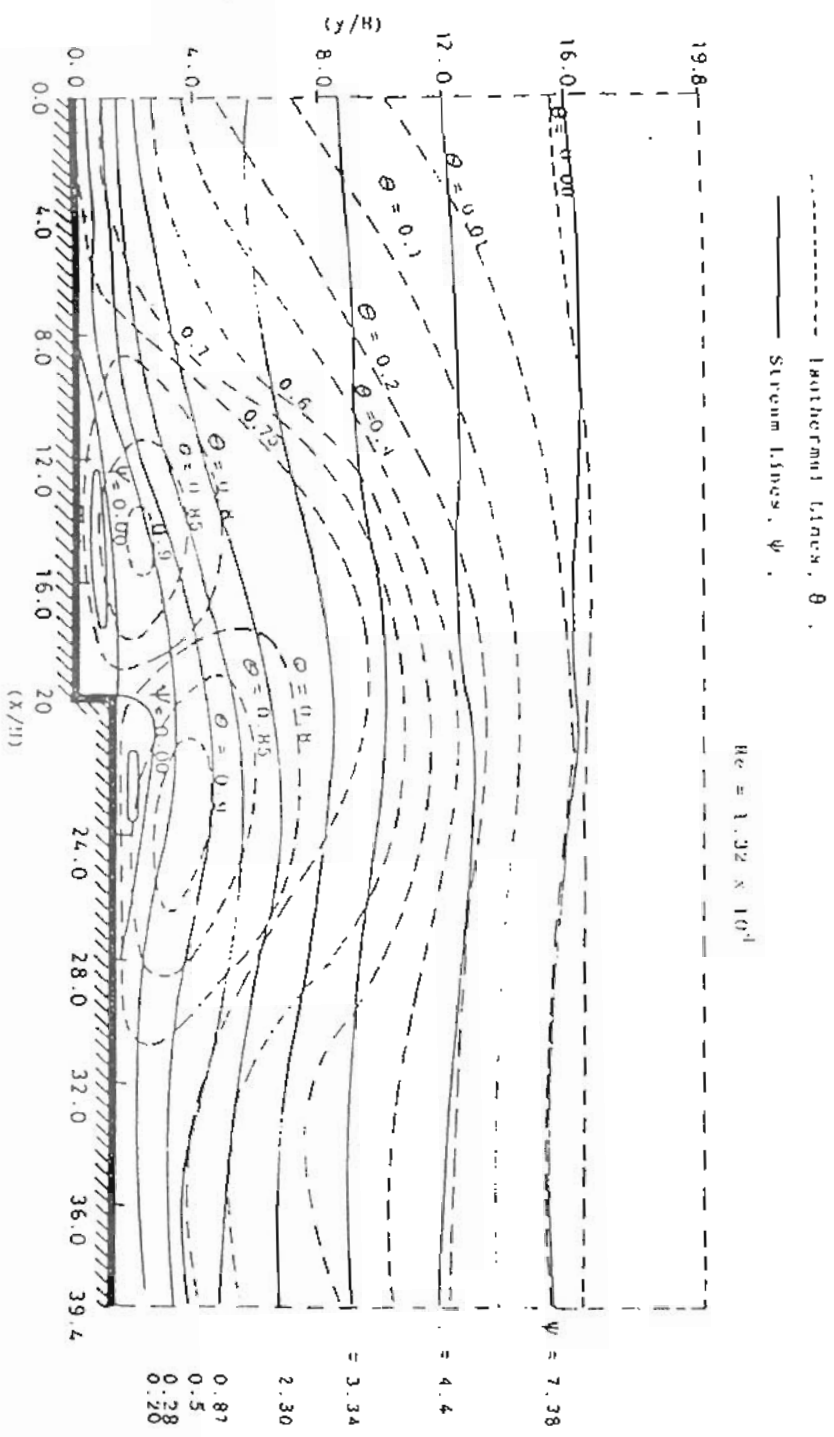


Fig. 3. Isothermal lines and stream lines distribution for  $Re = 1.32 \times 10^4$ ,  $H/Y_1 = 0.051$

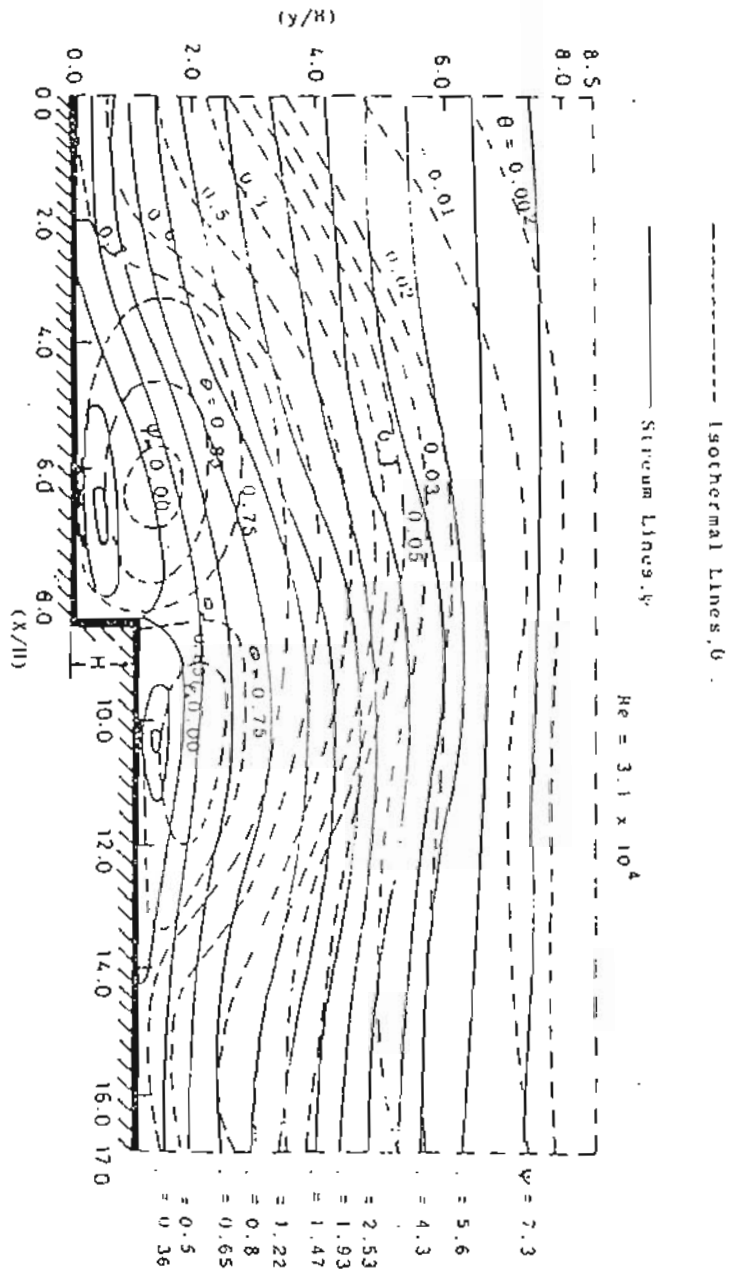


Fig. 4. Isothermal lines and stream lines distribution for  $Re = 3.1 \times 10^4$  ,  $H/Y_1 = 0.118$

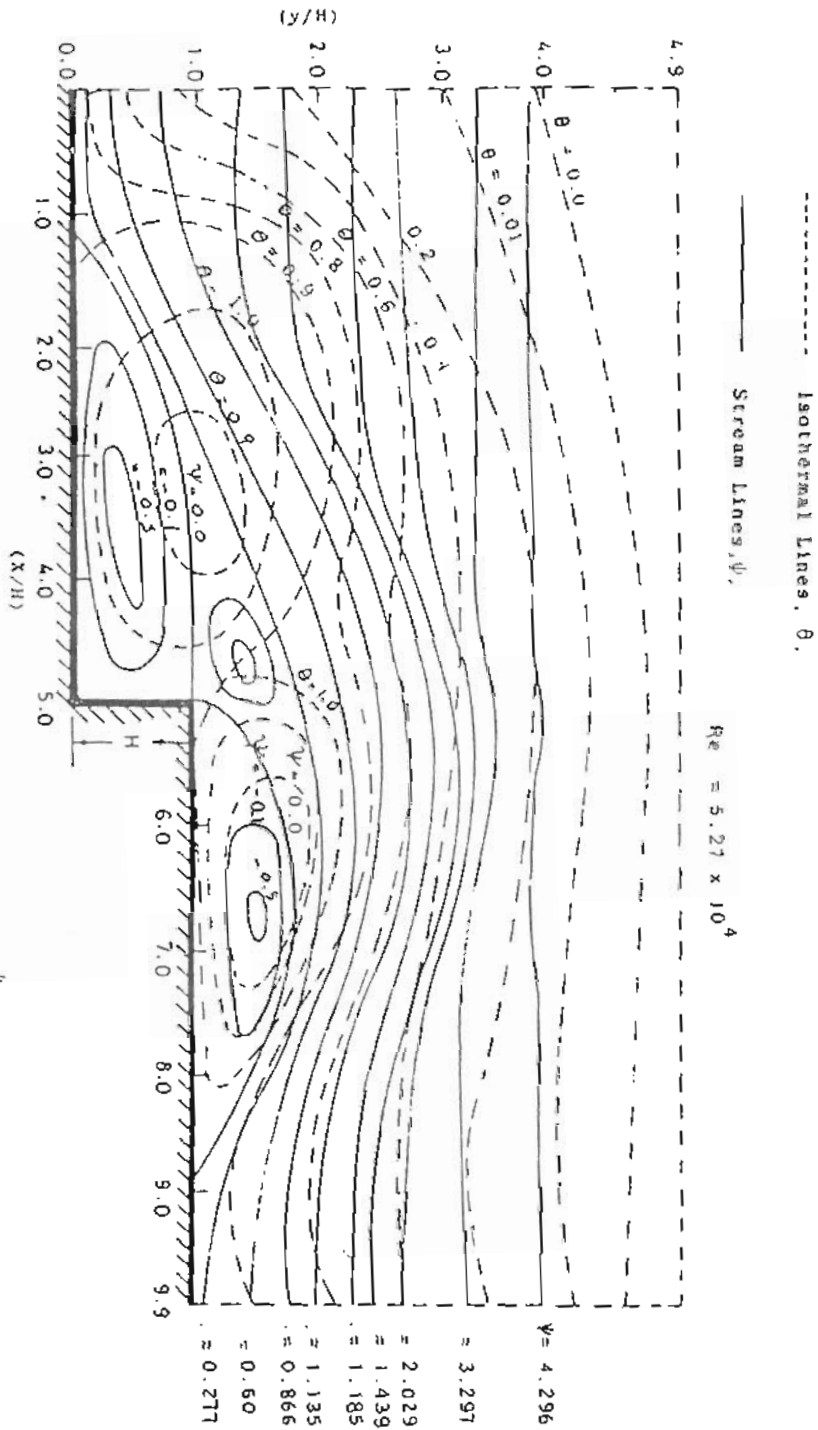


Fig. 5. Isothermal lines and Stream lines distribution for  $Re = 5.27 \times 10^4$  ,  $H/Y_1 = 0.203$

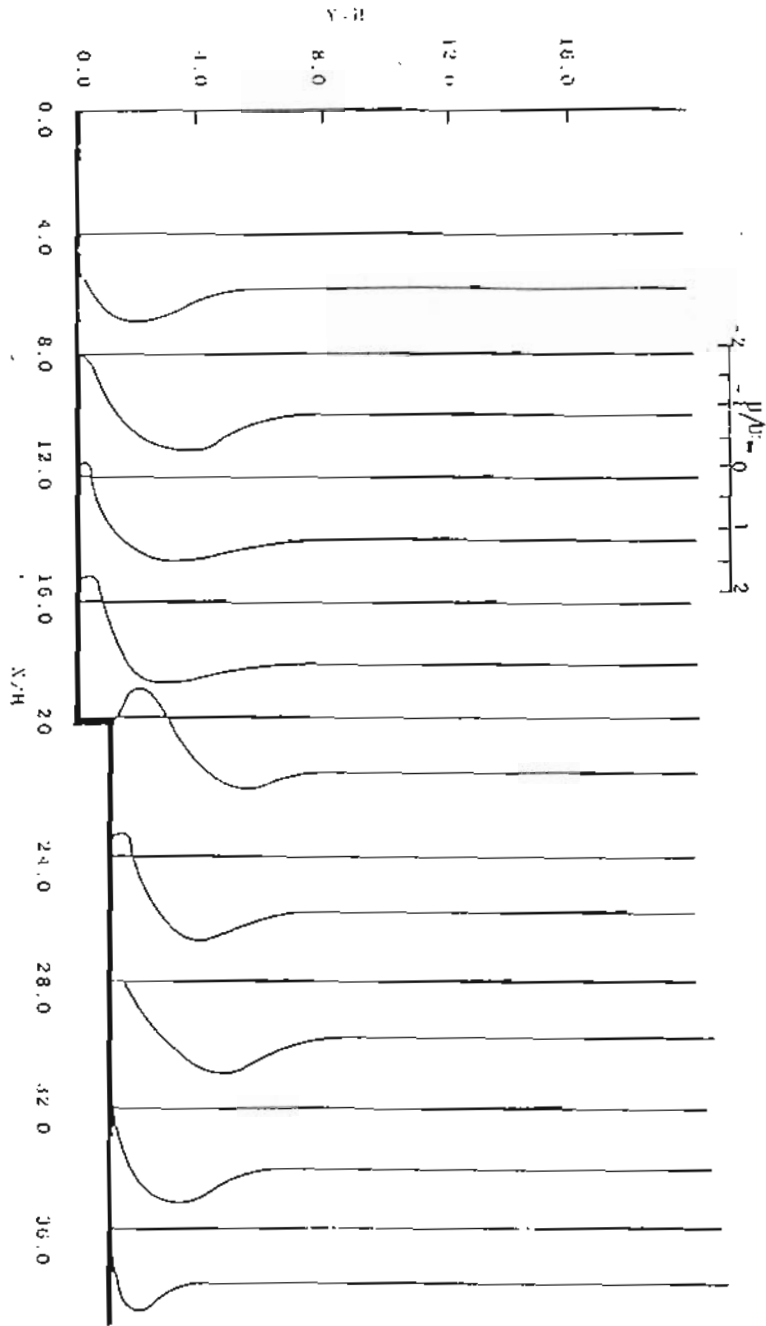


Fig. 6. Velocity distribution  $u/U_{\infty}$  for  $Re = 1.32 \times 10^4$  ,  $H/Y_1 = 0.051$

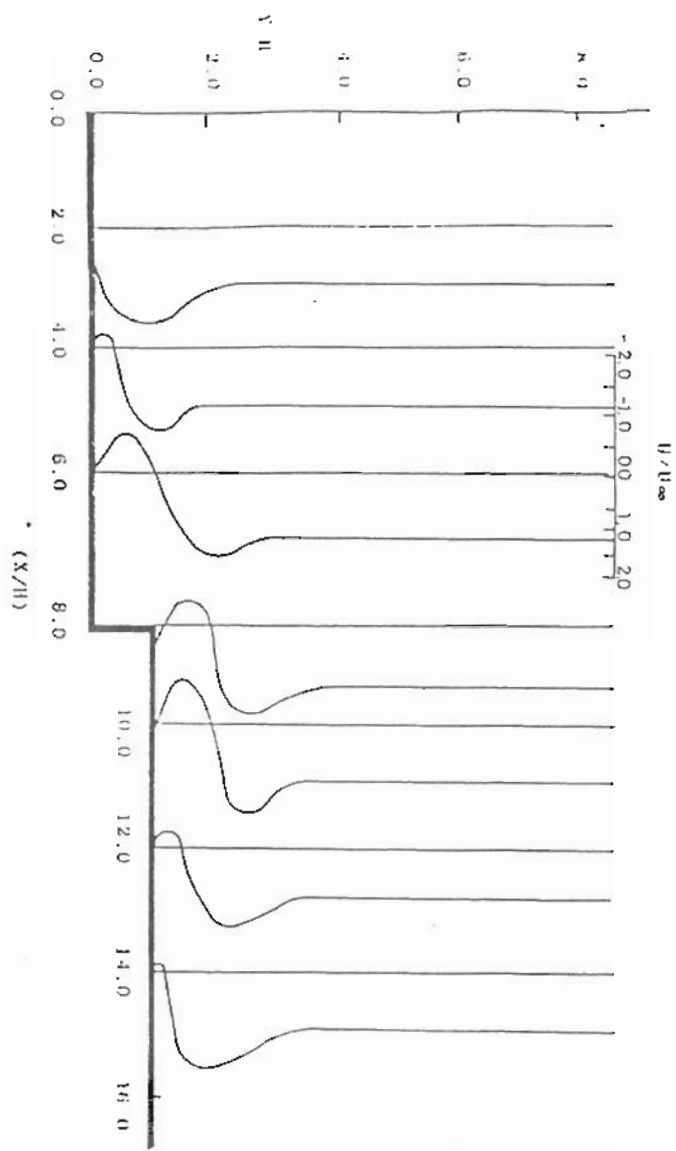


Fig. 7. Velocity distribution  $u/U_{\infty}$  for  $Re = 3.1 \times 10^4$ ,  $H/Y_1 = 0.118$

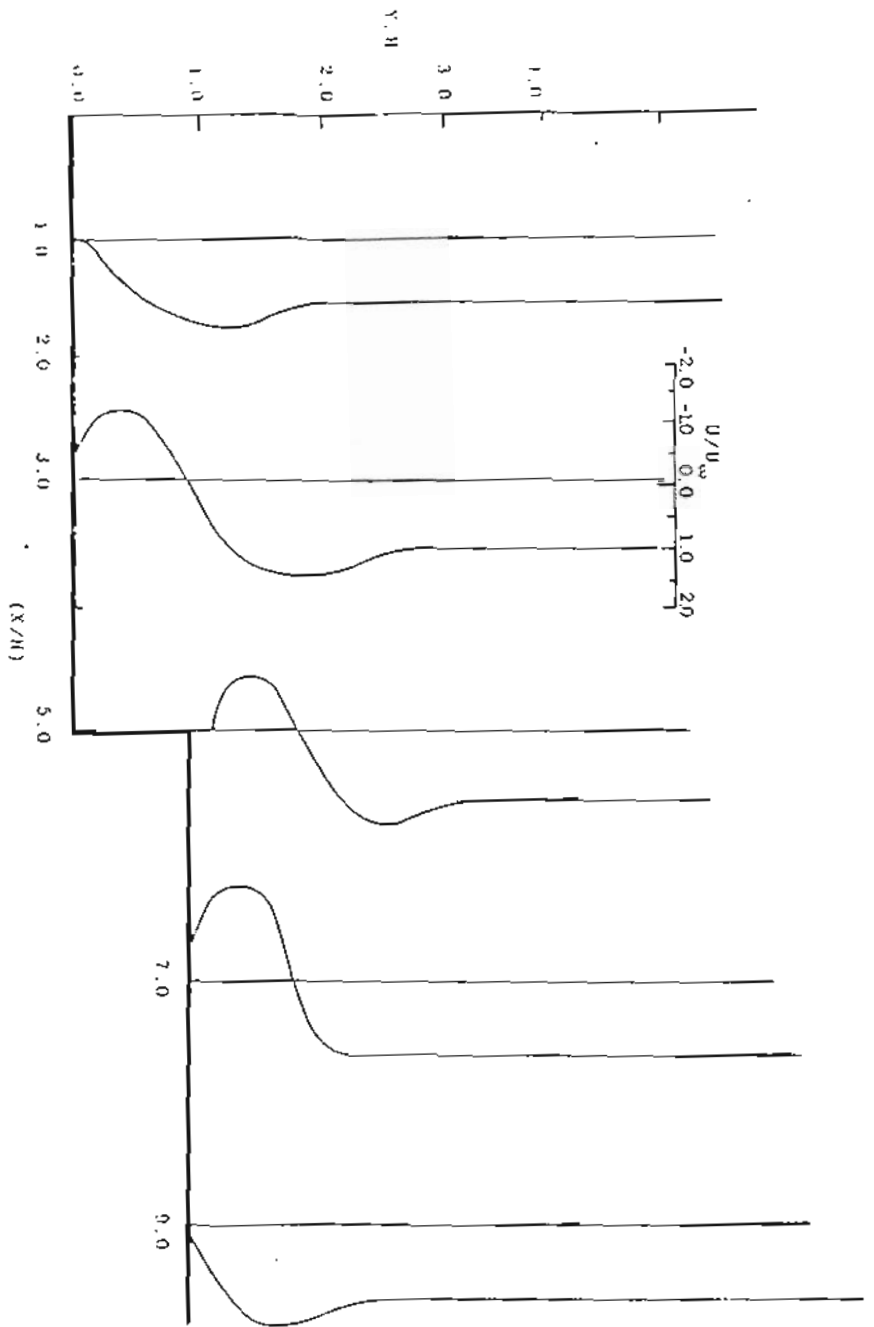


Fig. 8. Velocity distribution  $u/U_\infty$  for  $Re = 5.27 \times 10^4$  ,  $H/Y_1 = 0.203$



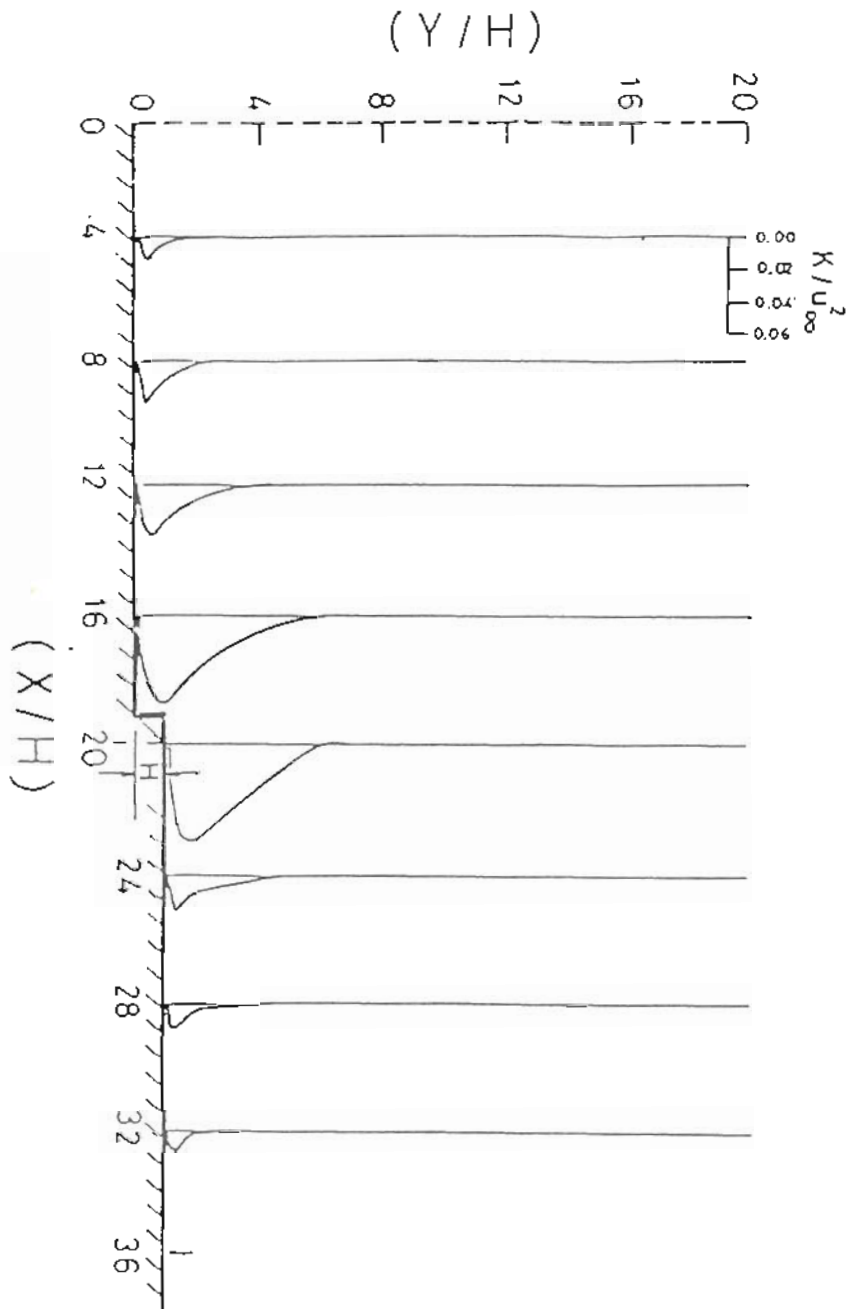


Fig. 9. Distribution of the kinetic energy for  $RE = 0.66 \times 10^4$  ,  $H/Y_1 = 0.051$

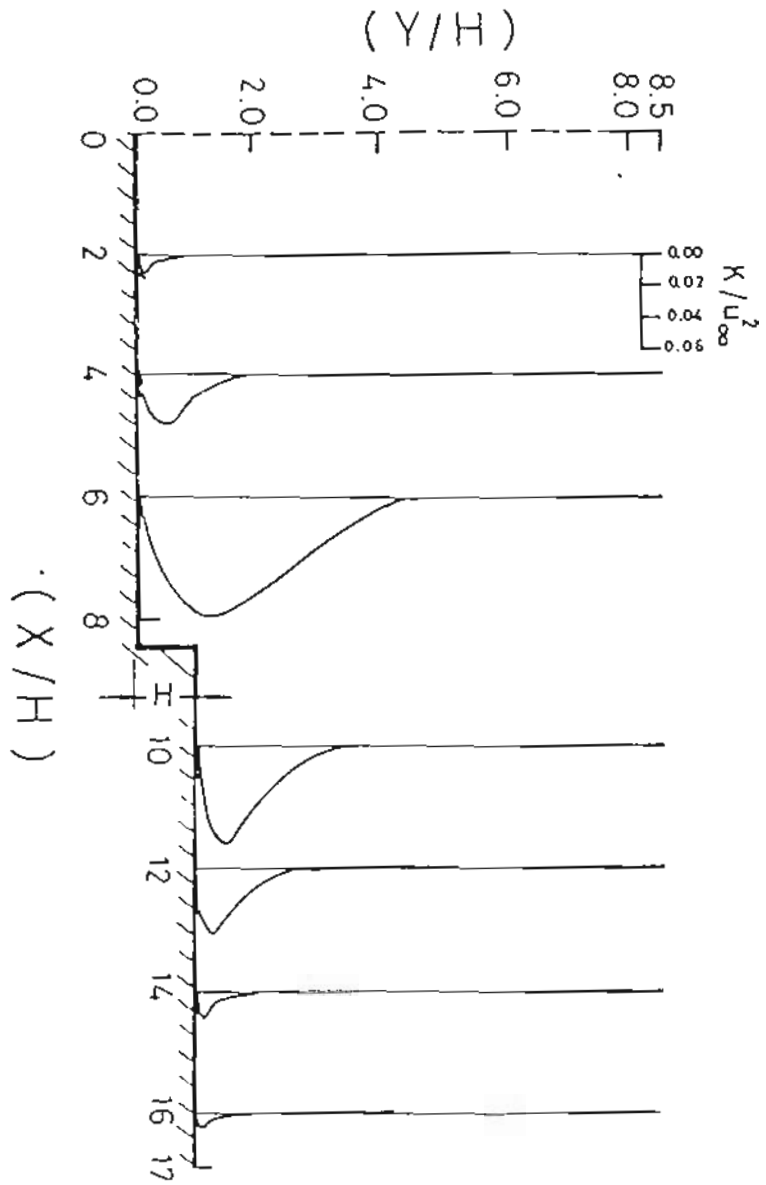


Fig. 10. Distribution of the kinetic energy for  $Re = 3.1 \times 10^4$  ,  $H/Y_1 = 0.118$

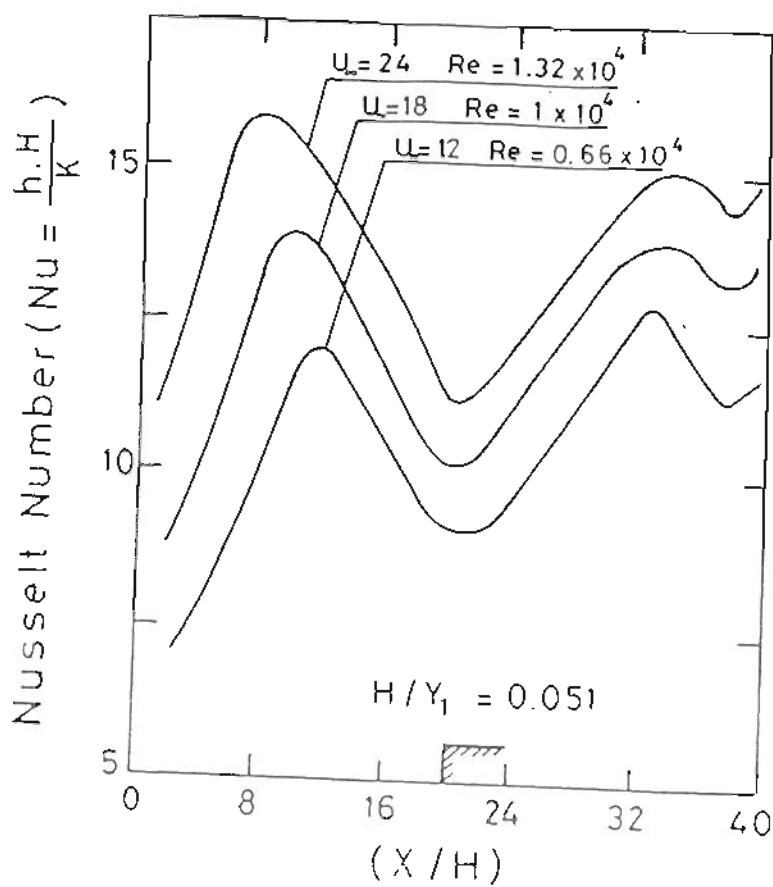


Fig. 11. Heat transfer coefficient patterns for different Reynolds numbers,  $H/Y_1 = 0.051$

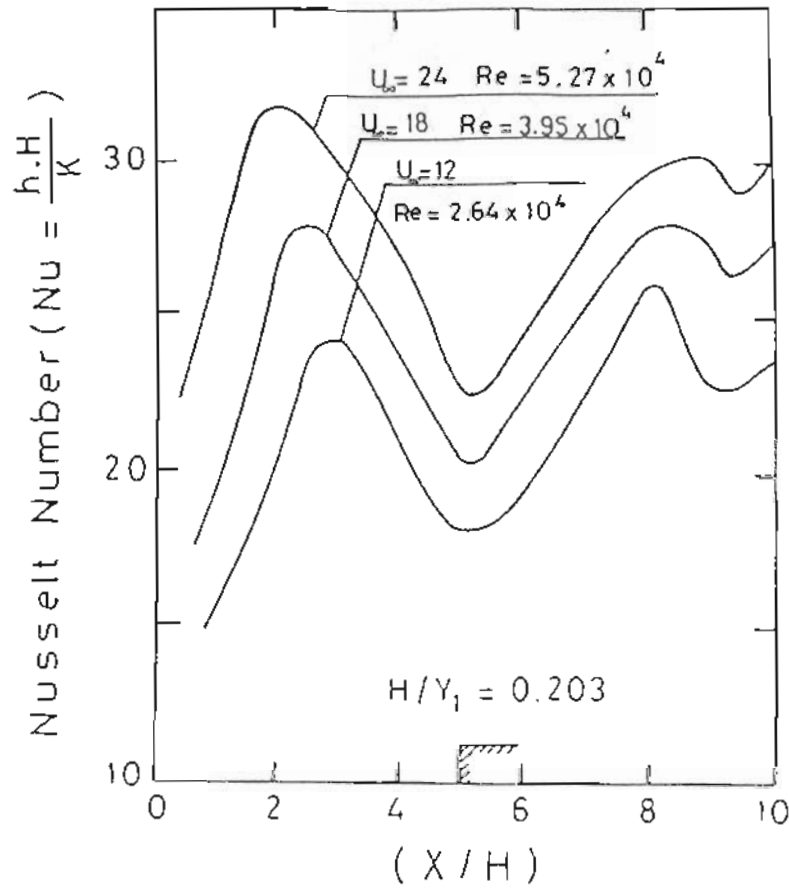


Fig. 12. Heat transfer coefficient patterns for different Reynolds numbers,  $H/Y_1 = 0.203$